2016/02/29

Dust formation and ejection by supernovae

Takaya Nozawa

(National Astronomical Observatory of Japan)

Contents:

- Introduction
- Production of dust in the ejecta of supernovae
- Ejection of dust from the supernova remnants
- Formation and survival of presolar grains

1-1. Introduction

○ Supernovae (SNe) are major sources of dust?

- abundant metal (metal : N > 5)
- low temperature (T < ~2000 K)
- high density (n_i > ~10^6 cm^{-3})

➔

- mass-loss winds of AGB stars
- expanding ejecta of SNe

- contribution of dust mass from AGB stars and SNe

  N(SNe) / N(AGB stars) ~ 0.05-0.1 (Salpeter IMF)

  M_{dust} = 0.01-0.05 M_{sun} per AGB star (e.g., Zhukovska & Gail 2008)

  M_{dust} = 0.1-1.0 M_{sun} per SN (e.g., Nozawa+2003, 2007)

- huge amounts of dust grains (>10^8 M_{sun}) at redshift z > 5

  ➔ 0.1 M_{sun} of dust per SN is needed to be ejected (Dwek+2007)

what composition, size, and mass of dust are ejected by SNe?

1-2. Summary of observed dust mass in CCSNe

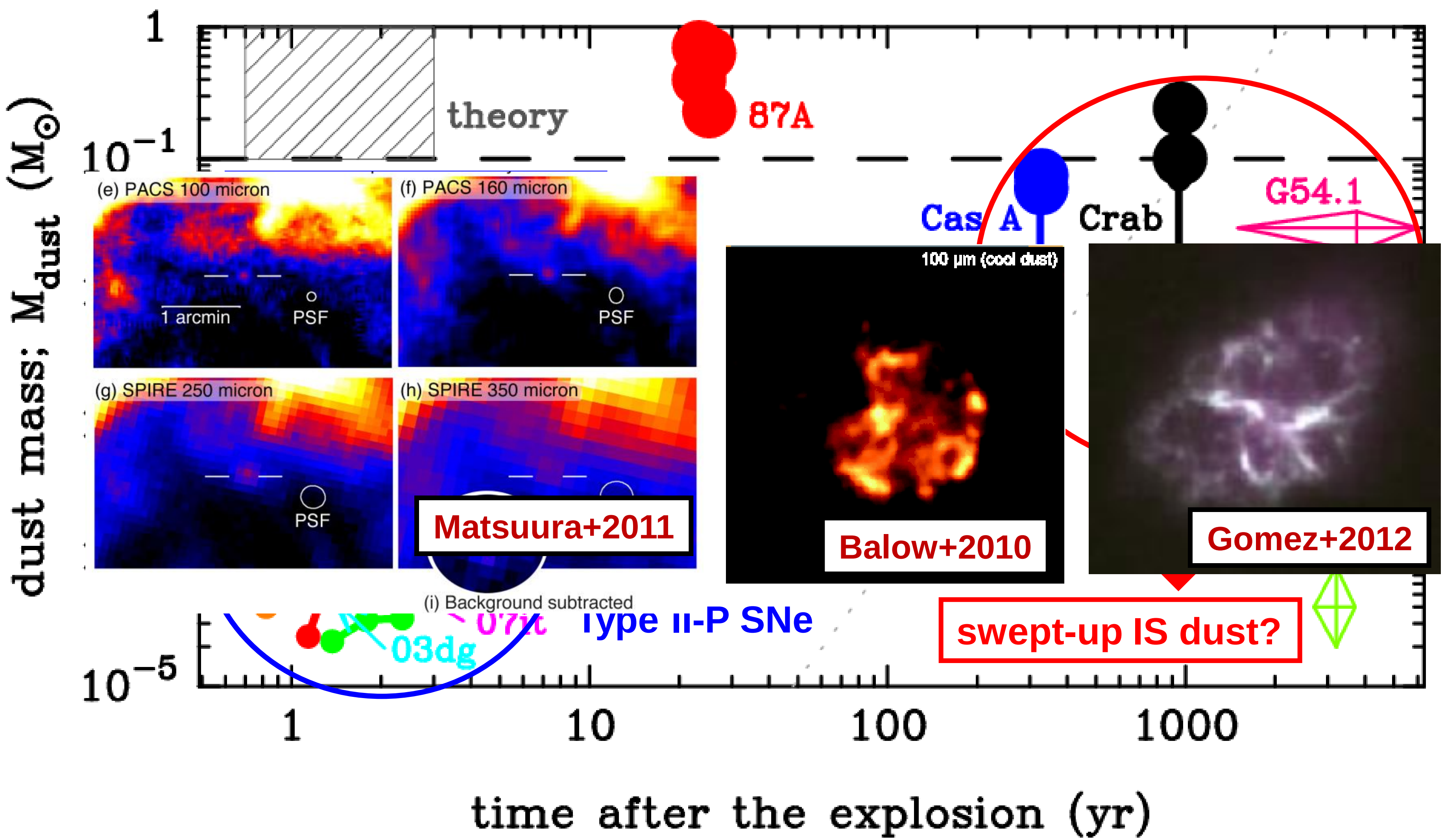

Far-IR to sub-mm observations are essential for revealing the mass of dust grains produced in the ejecta of SNe

1-2. Summary of observed dust mass in CCSNe

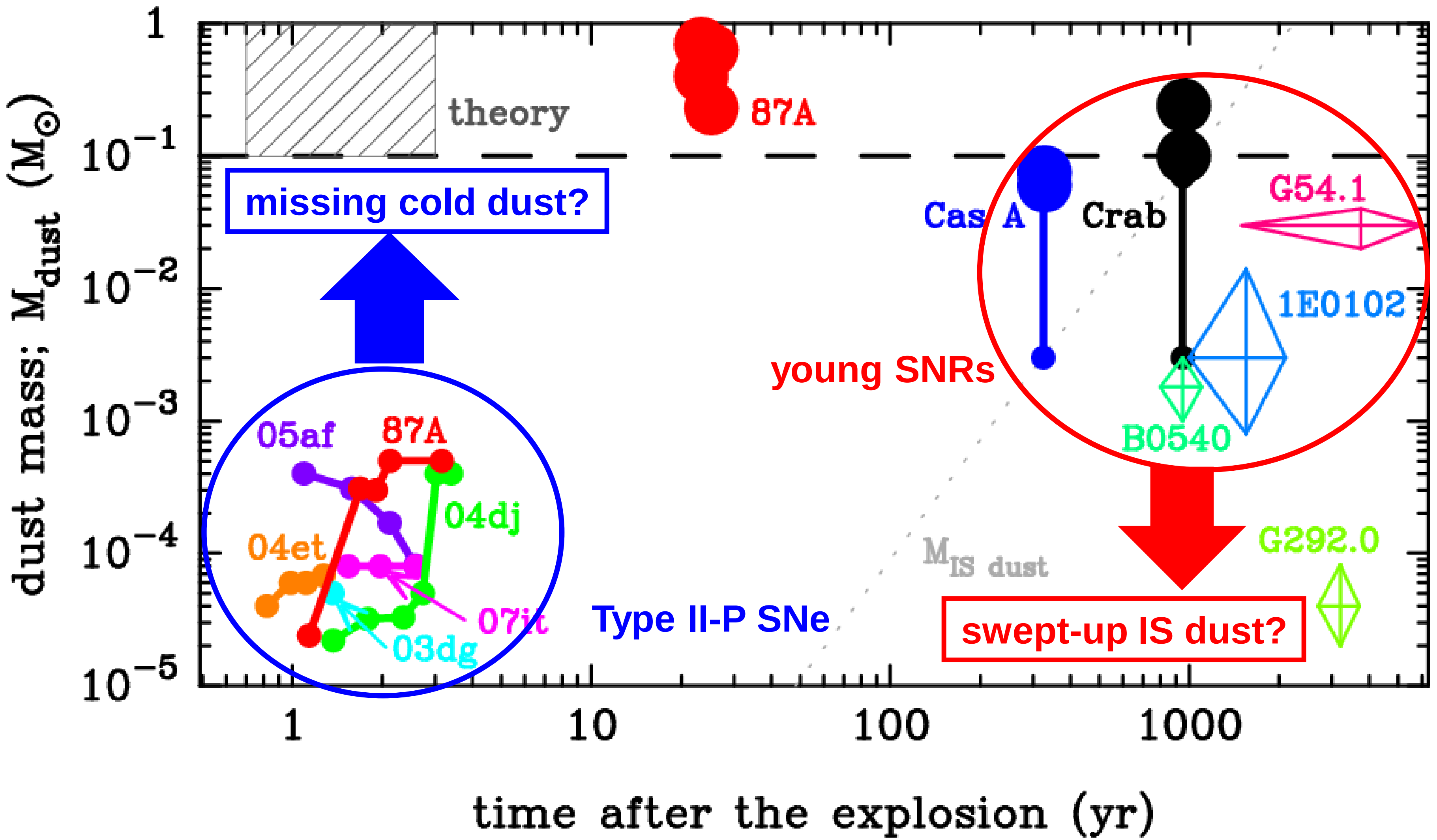

There are increasing pieces of evidence that massive dust in excess of 0.1 Msun is formed in the ejecta of SNe

1-3. Formation and processing of dust in SNe

Nozawa 2014, Astronomical Herald

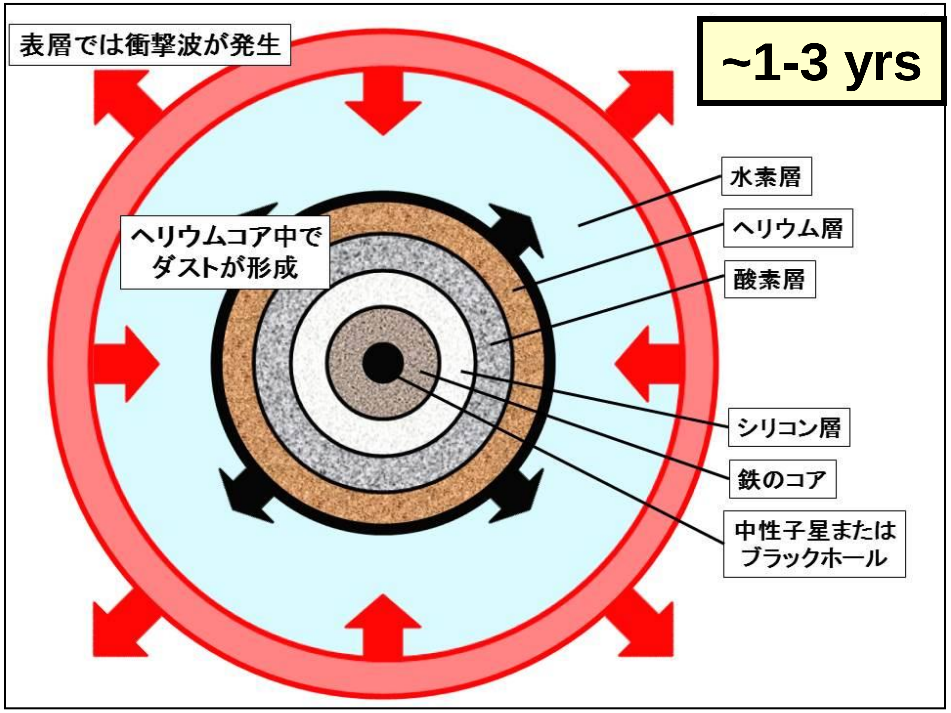

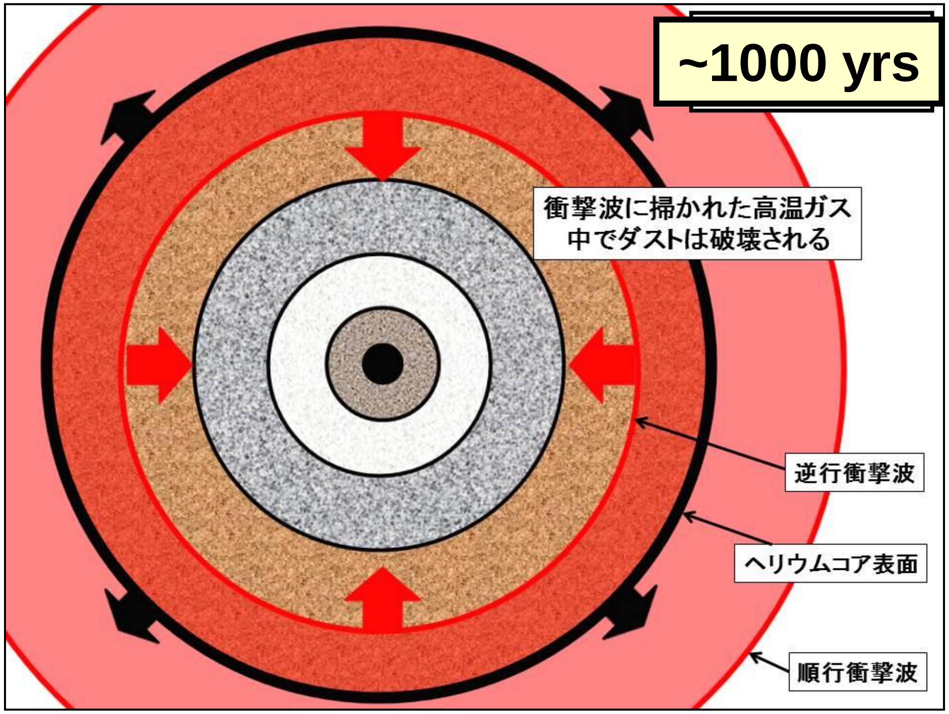

Destruction efficiency of dust grains by sputtering in the reverse shocks depends on their initial size

The size of newly formed dust is determined by physical condition (gas density and temperature) of SN ejecta

1-4. Achievement and issues on SN dust

○ What we have understood is

Core-collapse supernovae can produce a large amount of dust in excess of ~0.1 M_{sun} in the expanding ejecta

○ What we have not understood yet is

1) when the observed massive dust was formed?

➜ Cause of difference in dust mass in MIR and FIR

2) What composition and size distribution of dust are?

➜ Critical to the yield of dust finally ejected from SNe

2. Formation of dust in the ejecta of supernovae

2-1. Dust formation in Type II-P SNe

Nozawa+2003, ApJ, 598, 785

○ SN model (Population III SNe) **(Umeda & Nomoto 2002)**

- **SNe II : M_{ZAMS} = 13, 20, 25, 30 M_{sun} (E_{51}=1)**

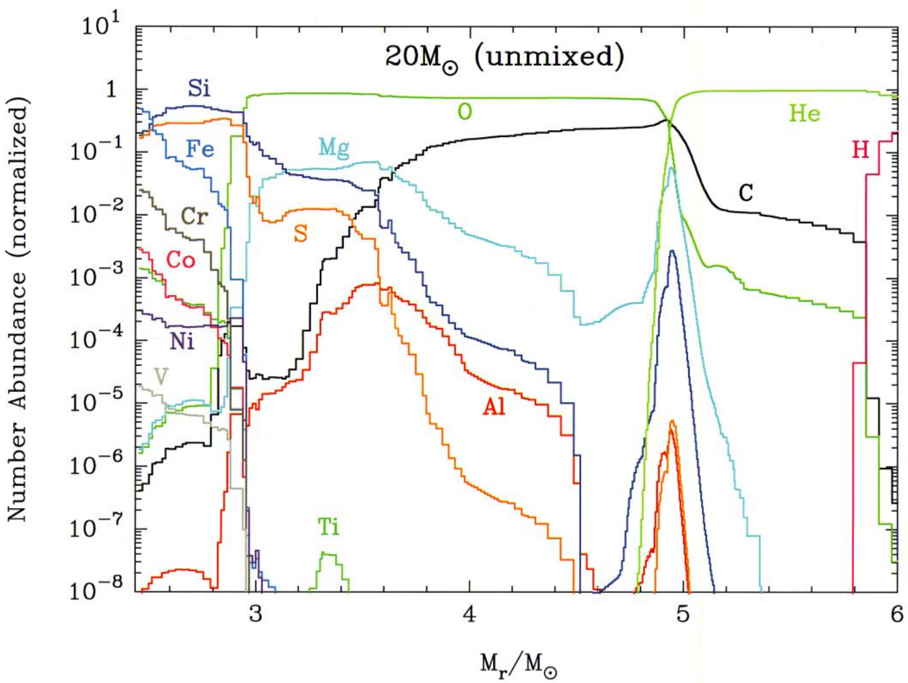

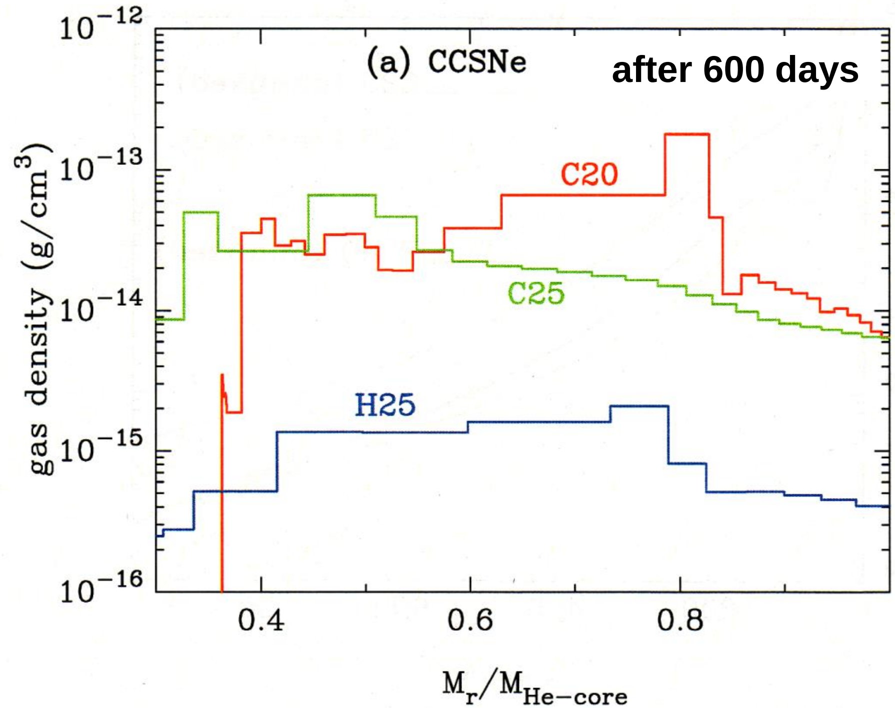

- **layered elemental distribution in the metal-rich He core**
- **no mixing of elements within the He-core**
- **gas density: ρ ~ 10^{-14}-10^{-13} g/cm3 ➜ n ~ 10^{8}-10^{10} /cm3**

2-2-1. Grain species considered in this study

○ dust formation theory

- nucleation
- grain growth

taking account of chemical reaction at condensation

key species：
gas species with the least collision frequency among reactants

key species controls the kinetics of the nucleation and grain growth

Dust species	Chemical reactions
$Fe_{(s)}$	$Fe_{(g)} \rightarrow Fe_{(s)}$
$FeS_{(s)}$	$Fe_{(g)} + S_{(g)} \rightarrow FeS_{(s)}$
$Si_{(s)}$	$Si_{(g)} \rightarrow Si_{(s)}$
$Ti_{(s)}$	$Ti_{(g)} \rightarrow Ti_{(s)}$
$V_{(s)}$	$V_{(g)} \rightarrow V_{(s)}$
$Cr_{(s)}$	$Cr_{(g)} \rightarrow Cr_{(s)}$
$Co_{(s)}$	$Co_{(g)} \rightarrow Co_{(s)}$
$Ni_{(s)}$	$Ni_{(g)} \rightarrow Ni_{(s)}$
$Cu_{(s)}$	$Cu_{(g)} \rightarrow Cu_{(s)}$
$C_{(s)}$	$C_{(g)} \rightarrow C_{(s)}$
$SiC_{(s)}$	$Si_{(g)} + C_{(g)} \rightarrow SiC_{(s)}$
$TiC_{(s)}$	$Ti_{(g)} + C_{(g)} \rightarrow TiC_{(s)}$
$Al_2O_{3(s)}$	$2Al_{(g)} + 3O_{(g)} \rightarrow Al_2O_{3(s)}$
$MgSiO_{3(s)}$	$Mg_{(g)} + SiO_{(g)} + 2O_{(g)} \rightarrow MgSiO_{3(s)}$
$Mg_2SiO_{4(s)}$	$2Mg_{(g)} + SiO_{(g)} + 3O_{(g)} \rightarrow Mg_2SiO_{4(s)}$
$SiO_{2(s)}$	$SiO_{(g)} + O_{(g)} \rightarrow SiO_{2(s)}$
$MgO_{(s)}$	$Mg_{(g)} + O_{(g)} \rightarrow MgO_{(s)}$
$Fe_3O_{4(s)}$	$3Fe_{(g)} + 4O_{(g)} \rightarrow Fe_3O_{4(s)}$
$FeO_{(s)}$	$Fe_{(g)} + O_{(g)} \rightarrow FeO_{(s)}$

2-2-2. Nucleation rate

Steady-state nucleation rate: Js

$$J_s(t) = \alpha_s \Omega \left(\frac{2\sigma}{\pi m_1} \right)^{\frac{1}{2}} \Pi c_1^2(t) \exp \left[-\frac{4}{27} \frac{\mu^3}{(\ln S)^2} \right]$$

Supersaturation ratio: S

$$\ln S = \ln \left(\frac{p_1}{\mathring{p}_1} \right) = -\frac{1}{kT} \left(\mathring{g}_s - \mathring{g}_1 \right) + \ln \left(\frac{p_1}{p_0} \right)$$

α_s : sticking probability of key species ($\alpha_s = 1$, in the calculations)

Ω : volume of the condensate per key species ($\Omega = 4\pi a_0^3/3$)

σ : surface energy of the condensate

m_1 : mass of key species

$c_1(t)$: number density of key species

μ : $\mu \equiv 4\pi a_0^2 \sigma / kT$; energy barrier for nucleation

2-2-3. Basic equations for dust formation

▪ Equation of mass conservation

$$c_{10} - c_1 = \int_{t_0}^{t} J_{n_*}(t') \frac{a^3(t,t')}{a_0^3} dt',$$

▪ Equation of grain growth

$$\frac{da}{dt} = s\Omega_0 \left(\frac{kT}{2\pi m_1} \right)^{\frac{1}{2}} c_1 \left(1 - \frac{1}{S} \right),$$

$$\frac{dV}{dt} = s\Omega_0 \, 4\pi a^2 \left(\frac{kT}{2\pi m_1} \right)^{\frac{1}{2}} c_1 \left(1 - \frac{1}{S} \right),$$

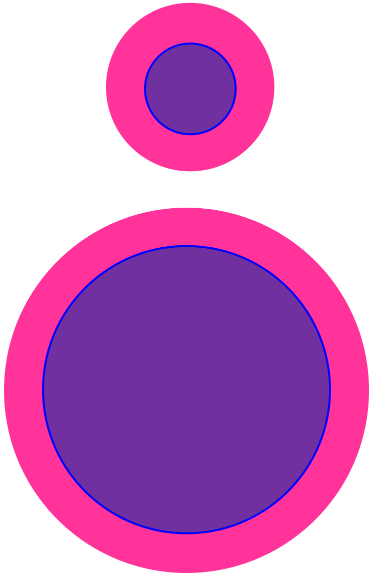

Growth rate is independent of grain radius

2-3. Dust formed in Type II-P SNe

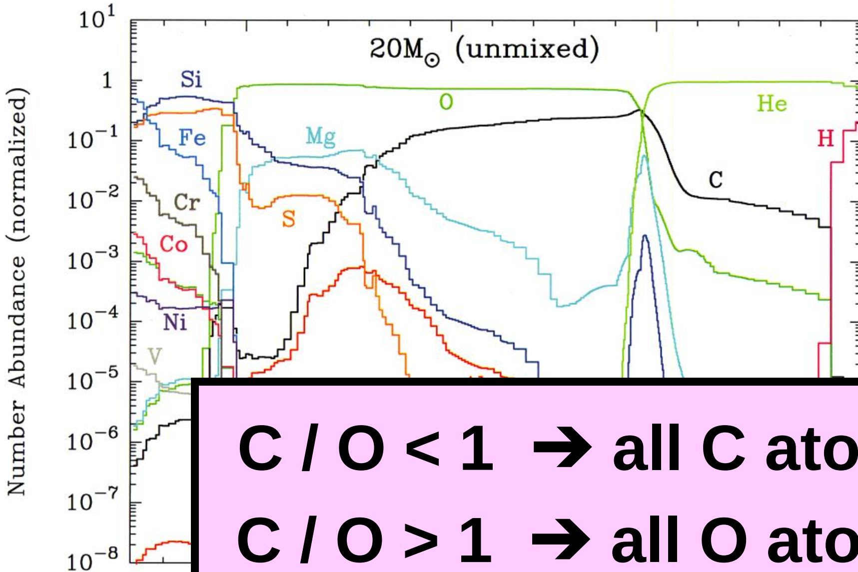

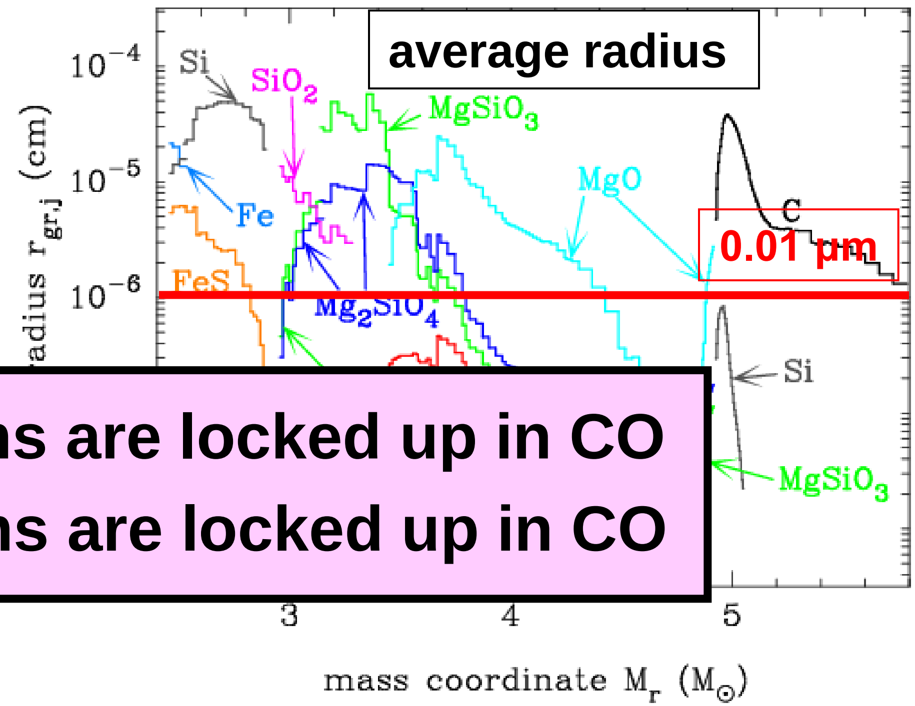

C / O < 1 ➔ all C atoms are locked up in CO

C / O > 1 ➔ all O atoms are locked up in CO

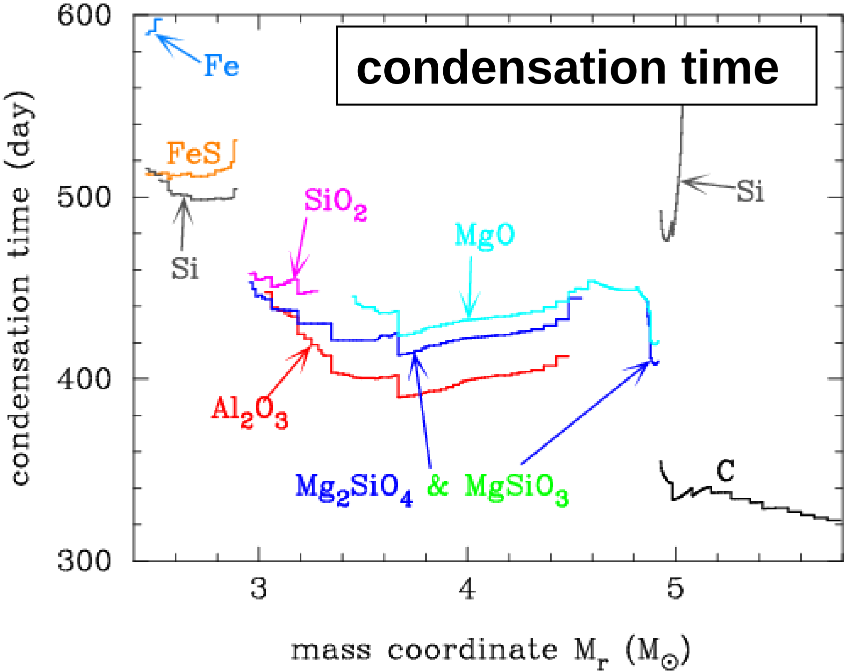

- a variety of grain species can condense according to elemental composition in each layer
- condensation time: 300-600d after explosion
- average grain radii: >~0.01 μm

Nozawa+03, ApJ, 598, 785

2-4. Size distribution of newly formed dust

Nozawa+2003, ApJ, 598, 785

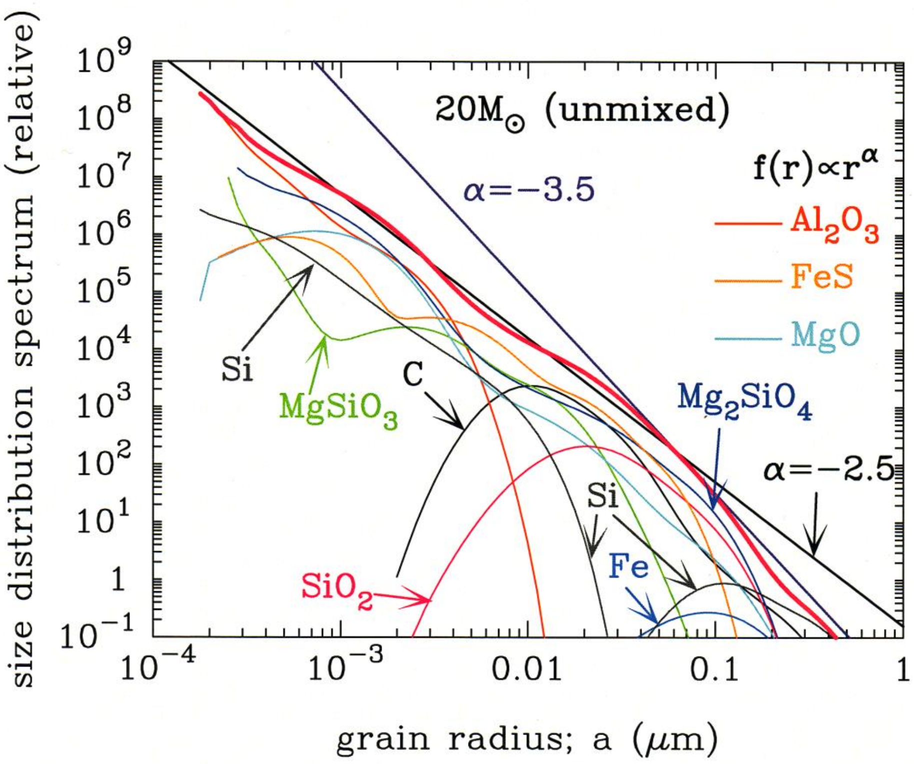

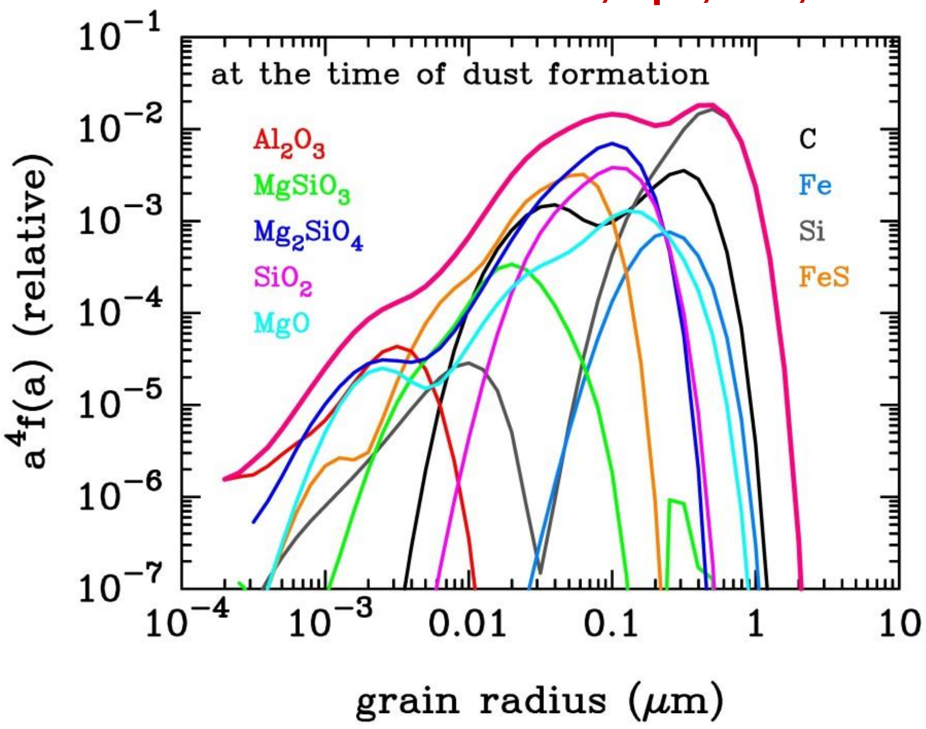

- C, SiO2, and Fe grains have lognormal-like size distribution, while the other grains have power-law size distribution
- Size distribution summed up over all grain species is roughly described by a broken power-law with the index of -2.5 and -3.5
- Size distribution of dust in mass has a peak around 0.1-1 μm

3. Destruction of dust grains by SN reverse shocks

$T = (1\text{-}2)\text{x}10^4$ K
$n_{H,0} = 0.1\text{-}1\ \text{cm}^{-3}$

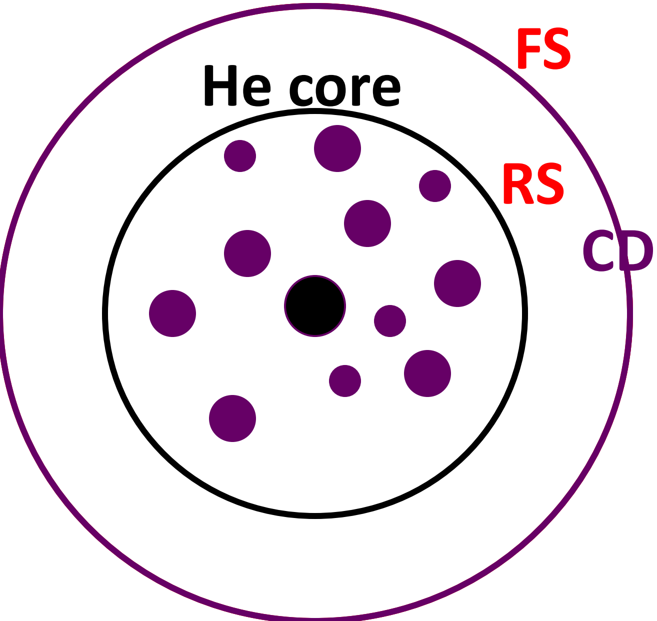

3-1-1. Time evolution of SNRs

- Basic equations (spherical symmetry)

$$\frac{\partial \rho}{dt} + \frac{1}{r^2}\frac{\partial}{\partial r}(r^2 \rho v) = 0$$

$$\frac{\partial}{dt}(\rho v) + \frac{1}{r^2}\frac{\partial}{\partial r}(r^2 \rho v^2) = -\frac{\partial P}{\partial r}$$

$$\frac{\partial}{dt}\left(\frac{\rho v^2}{2} + \frac{P}{\gamma - 1}\right) + \frac{1}{r^2}\frac{\partial}{\partial r}\left(r^2\left[\frac{\rho v^2}{2} + \frac{\gamma P}{\gamma - 1}\right] v\right)$$

$$= -(n_{\rm e} n_{\rm H} \Lambda_{\rm gas}(T) + \Lambda_{\rm ic}(T) + \Lambda_{\rm d}(n_{\rm H}, T))$$

$\Lambda_{\rm gas}(T)$: cooling function of gas by the atomic process (Sutherland & Dopita 1993; Smith et al. 2001)

$\Lambda_{\rm ic}(T)$: inverse Compton cooling (Ikeuchi & Ostriker 1986)

$\Lambda_{\rm ic}(T) = 5.41 \times 10^{-32} (1+z)^4 n_e (T/10^4\ {\rm K})$ (we adopt $z = 20$)

$\Lambda_{\rm d}(n_{\rm H}, T)$: cooling of gas through thermal emission of dust

· numerical code : flux splitting method (van Albada et al. 1982)

3-1-2. Dynamics of dust

- deceleration of dust due to drag force (Baines et al. 1965)

$$\frac{dw_{\rm d}}{dt} = \frac{F_{\rm drag}}{m_{\rm d}} = -\frac{3n_{\rm H}kT}{2a\rho_{\rm d}}\sum_i A_i G_i(s_i) \quad (w_{\rm d} : \text{relative velocity})$$

$$\begin{aligned} F_{\rm drag} &= m_{\rm d}\frac{dw_{\rm d}}{dt} = -\pi a^2 \sum n_i \langle v_i m_i v_i \cos\theta \rangle \\ \frac{dw_{\rm d}}{dt} &= -\frac{\pi a^2}{\frac{4}{3}\pi a^3 \rho_d} n_{\rm H} \sum A_i \langle v_i m_i v_i \cos\theta \rangle \\ &= -\frac{3n_{\rm H}}{4a\rho_d} kT \sum A_i G_i \end{aligned}$$

by $n_{\rm H}$

$$G_i(s_i) \approx \frac{8s_i}{3\sqrt{\pi}}\left(1 + \frac{9\pi}{64}s_i^2\right)^{\frac{1}{2}} \quad \text{(Draine \& Salpeter 1979)}$$

where $s_i^2 = m_i w_{\rm d}^2 / 2kT$

3-1-3. Erosion rate of dust by sputtering

• dust destructio … 996)

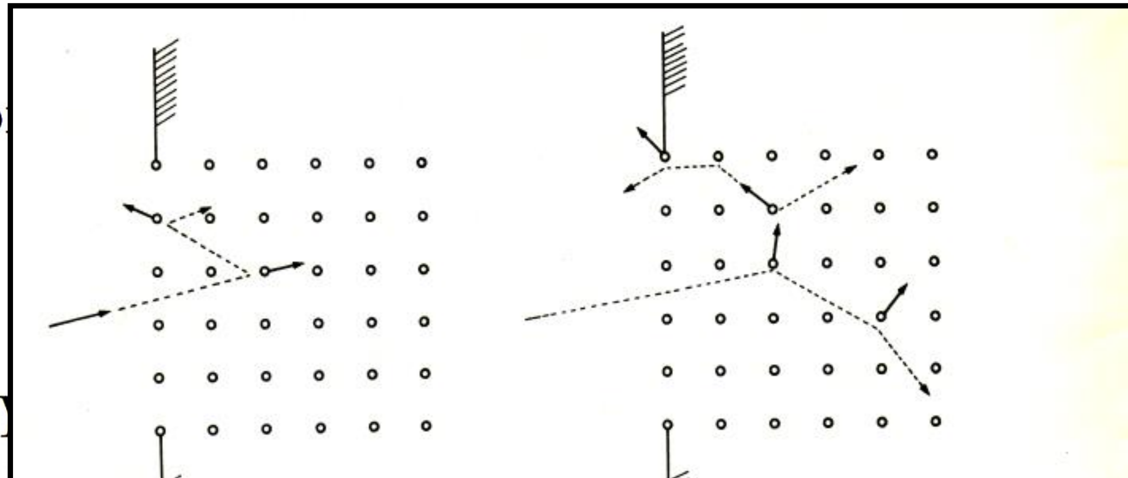

$Y_i(E) = 2$ …

· rate … s taken

acco …

$\mathcal{R}($ … $)X_i(\epsilon)d\epsilon$

w …

$$\frac{dV_{\rm d}}{dt} = 4\pi a^2 \frac{da}{dt} = -\pi a^2 \frac{4\pi a_0^3}{3} \sum n_i \langle v_i Y_i \rangle$$

$$\frac{da}{dt} = -\frac{1}{4} \Omega n_{\rm H} \sum A_i \langle v_i Y_i \rangle$$

$$\frac{da}{dt} = -\frac{m_{\rm sp}}{2\rho_{\rm d}} n_{\rm H} \sum A_i \left(\frac{8kT}{\pi m_i}\right)^{1/2} \frac{e^{-s_i^2}}{2s_i} \times \int \epsilon^{\frac{1}{2}} e^{-\epsilon_i} \sinh(2 s_i \epsilon_i^{\frac{1}{2}}) Y_i^0(\epsilon_i) d\epsilon_i$$

3-2. Temperature and density of gas in SNRs

Nozawa+07, ApJ, 666, 955

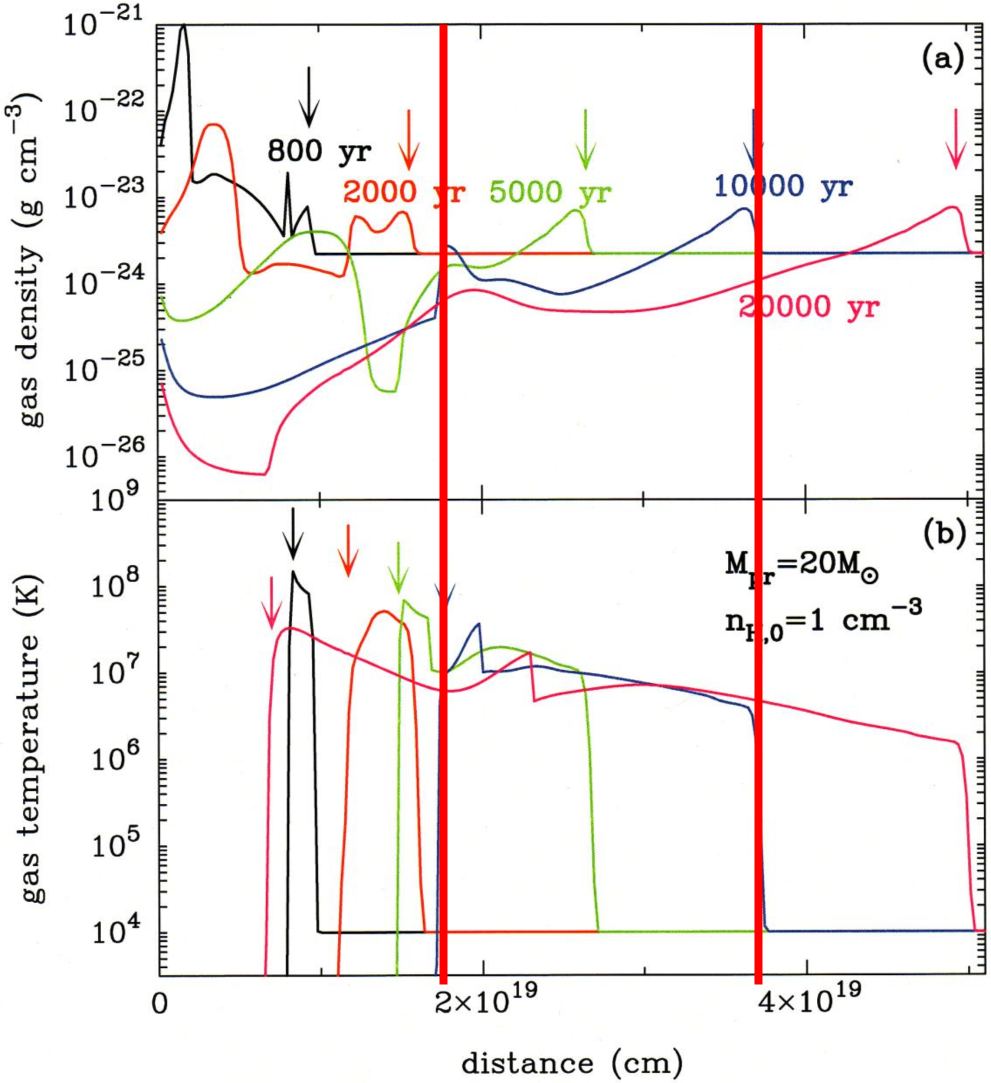

Model : M_{pr}= 20 Msun (E_{51}=1)
$n_{H,0}$ = 1 cm^{-3}

Downward-pointing arrows:
forward shock in upper panel
reverse shock in lower panel

The temperature of the gas swept up by the shocks
➔ 10^6-10^8 K
↓
Dust grains residing in the shocked hot gas are eroded by sputtering

3-3. Evolution of dust in SNRs

Model : M_{pr} = 20 M_{sun} (E_{51}=1), $n_{H,0}$ = 1 cm^{-3}

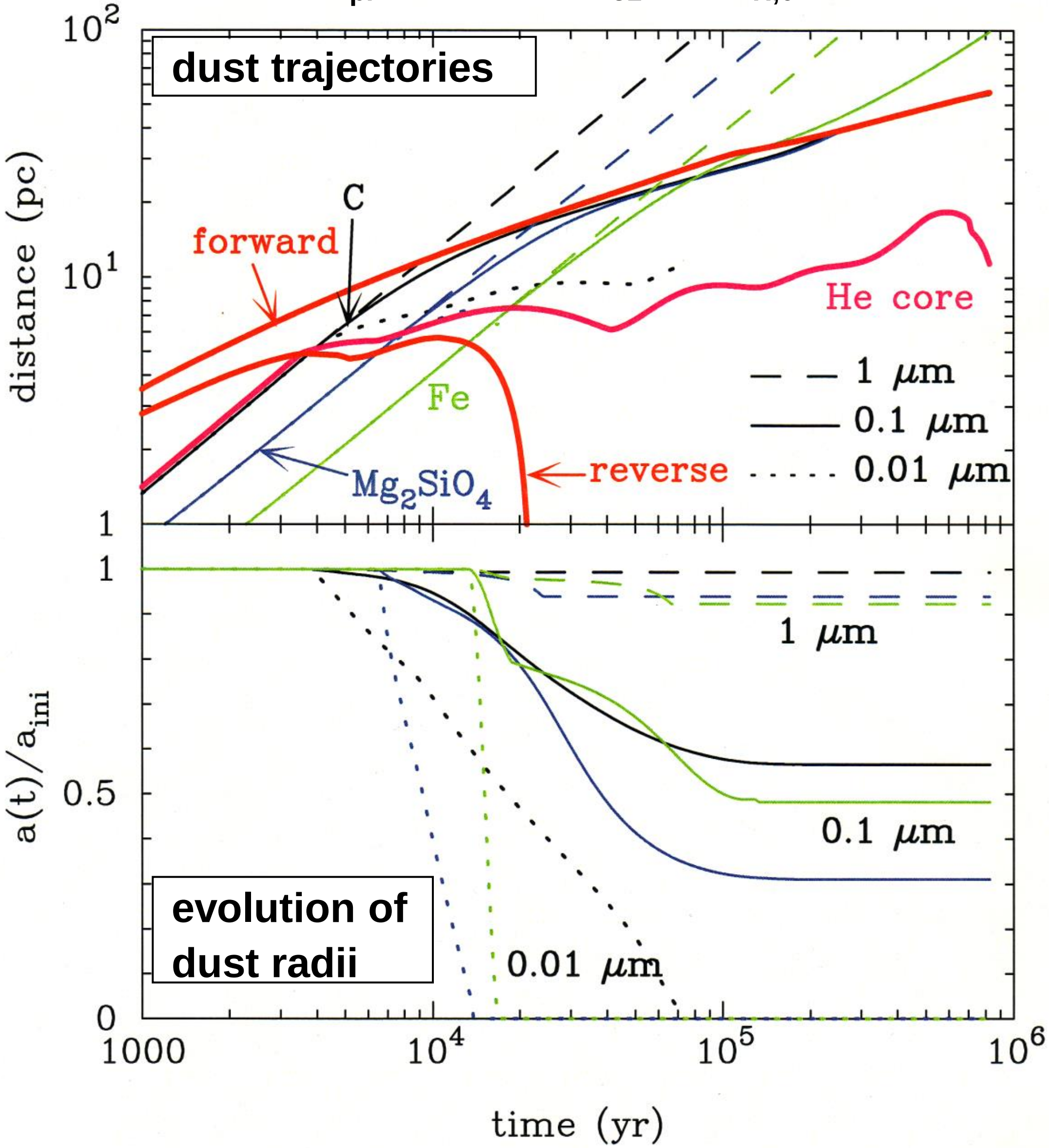

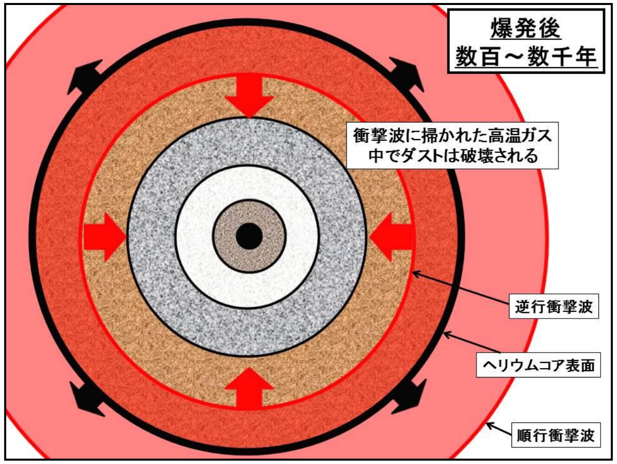

The evolution of dust heavily depends on the initial radius and composition

a_{ini} = 0.01 μm (dotted lines)
➔ completely destroyed

a_{ini} = 0.1 μm (solid lines)
➔ trapped in the shell

a_{ini} = 1 μm (dashed lines)
➔ injected into the ISM

Nozawa+07, ApJ, 666, 955

3-4. Dust mass and size ejected from SNe II

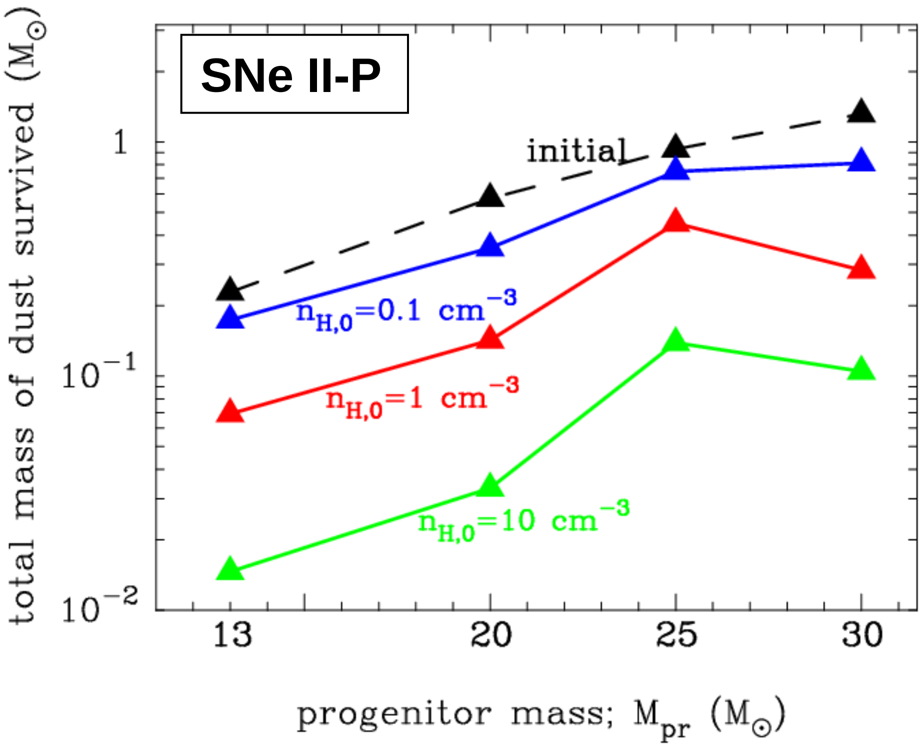

Nozawa+07, ApJ, 666, 955

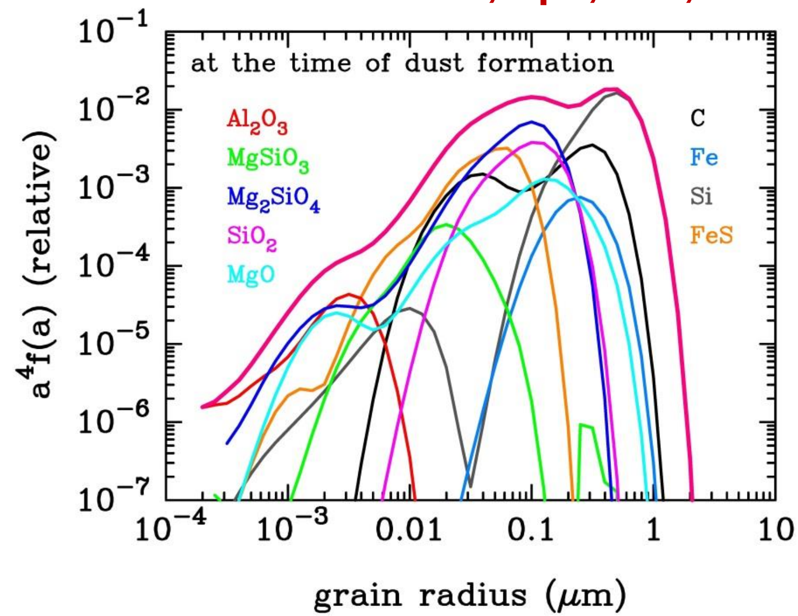

total mass of dust surviving the destruction in Type II SNRs;
0.07-0.8 Msun ($n_{H,0}$ = 0.1-1 cm^{-3})

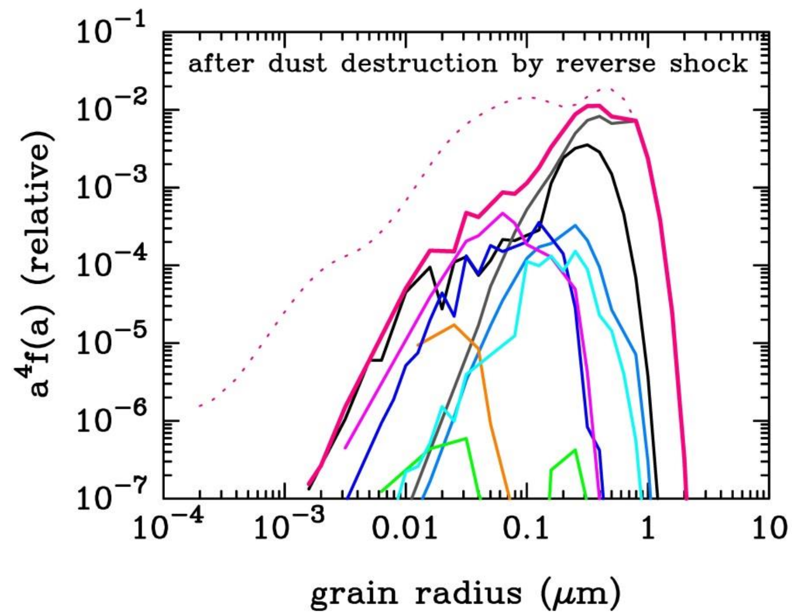

size distribution of dust after the shock-destruction is domimated by large grains (> 0.1 μm)

3-5. Conclusions from theoretical works

1) When the observed massive dust was formed?

➜ within 3 years after SN explosion

2) What composition and size distribution of dust are?

- **composition: carbon, silicate, oxide, pure iron …**

- **size (distribution)**
  - **at the formation ➜ a few A to ~1 μm (broken power-law)**
  - **after destruction ➜ biased to larger than ~0.1 μm**

- **dust mass**
  - **at the formation: 0.1-1.3 Msun**

    ➜ after destruction: 0.07-0.8 Msun

4. Formation and survival of presolar grains

4-1. No formation of SiC in the calculations

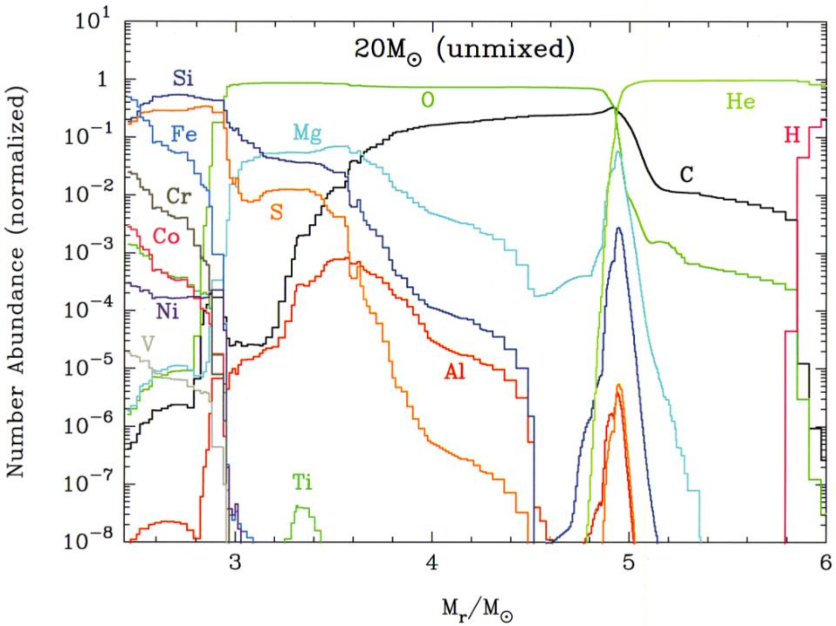

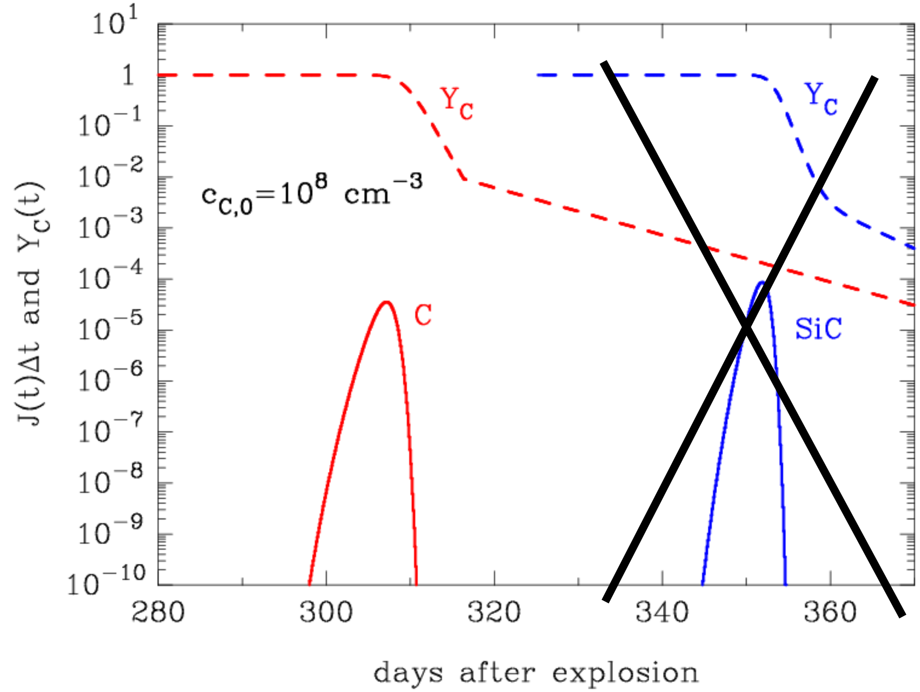

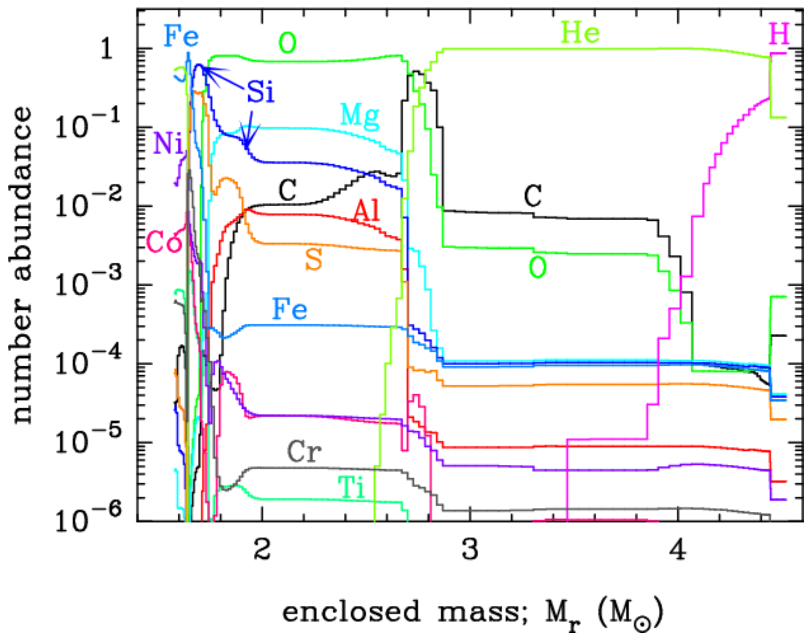

The earlier formation of C grains prevents condensation of SiC

4-2. Isotopic composition of presolar oxides

○ Oxygen isotopic composition of presolar oxide grains

presolar Al_2O_3 grains

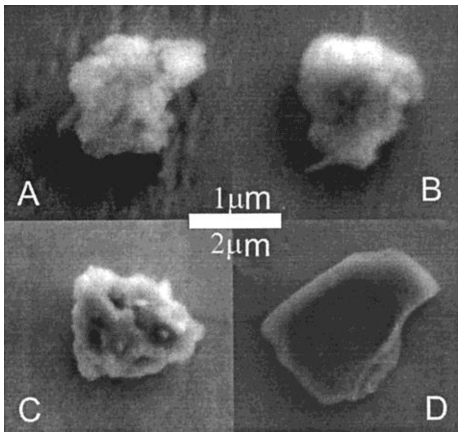

Choi+1998

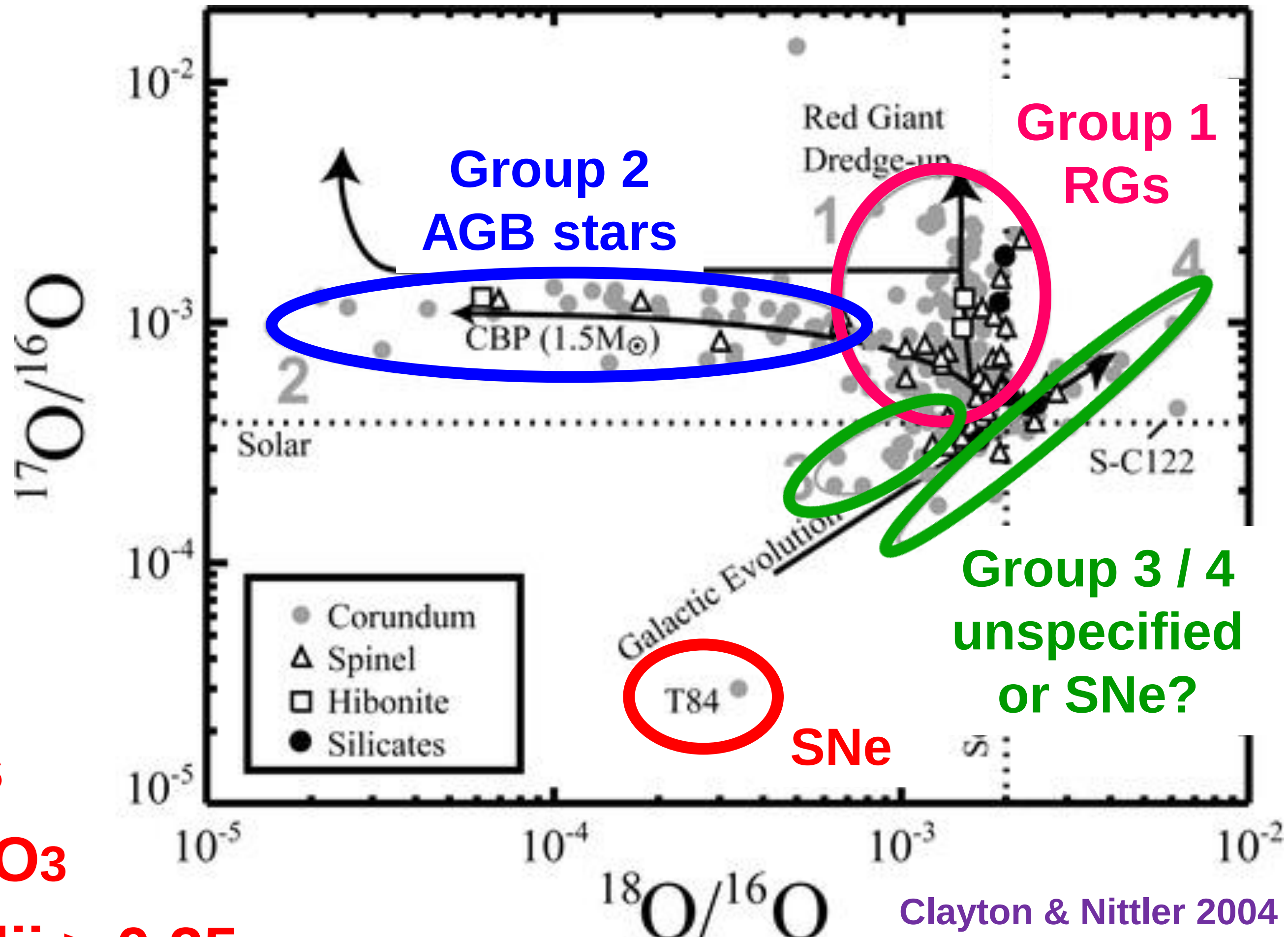

Clayton & Nittler 2004

A few particles of presolar Al_2O_3 grains with radii > 0.25 μm are believed to have been produced in the ejecta of SNe

4-3. Why we focus on presolar Al_2O_3 grains?

○ Evidence for Al_2O_3 formation in SNe

- Infrared spectra of Cassiopeia A (Cas A) SNR

  ➜ Al_2O_3 is one of the main grain species

  (Douvion et al. 2001; Rho et al. 2008)

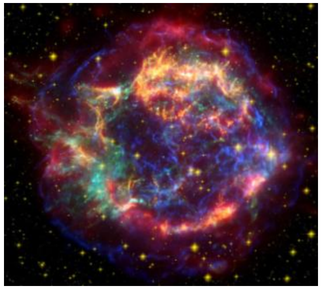

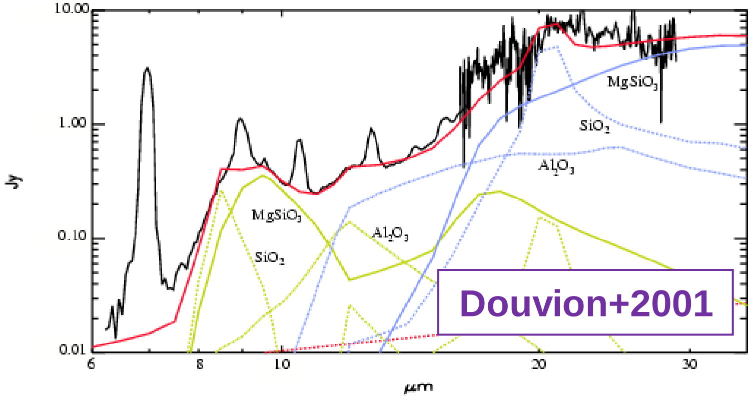

○ Dust formation calculations

- the first condensate among oxide

  ➜ sizes of Al_2O_3 grains : < ~0.03 μm

  (e.g., Nozawa+2003; Todini & Ferrara+2001)

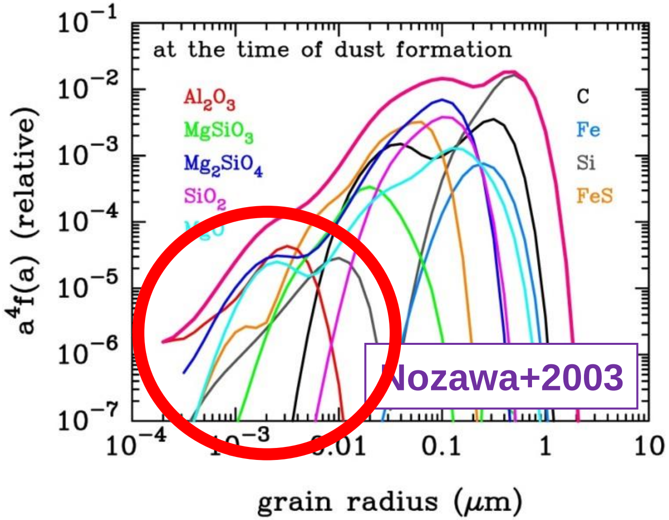

destruction in SNRs

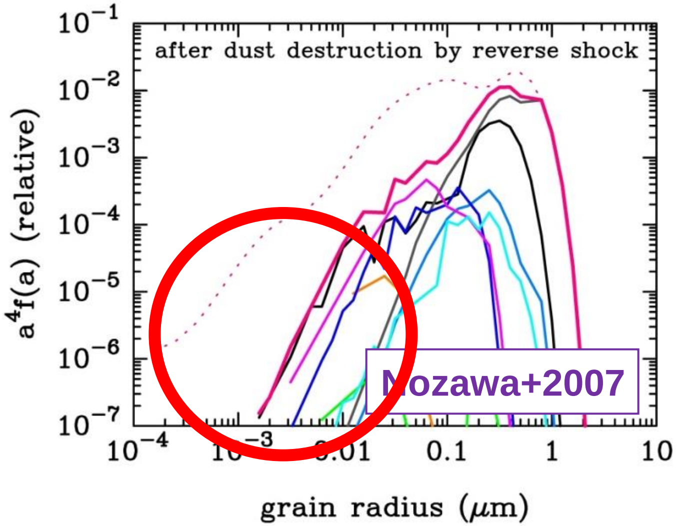

4-4. Formation condition of presolar Al_2O_3

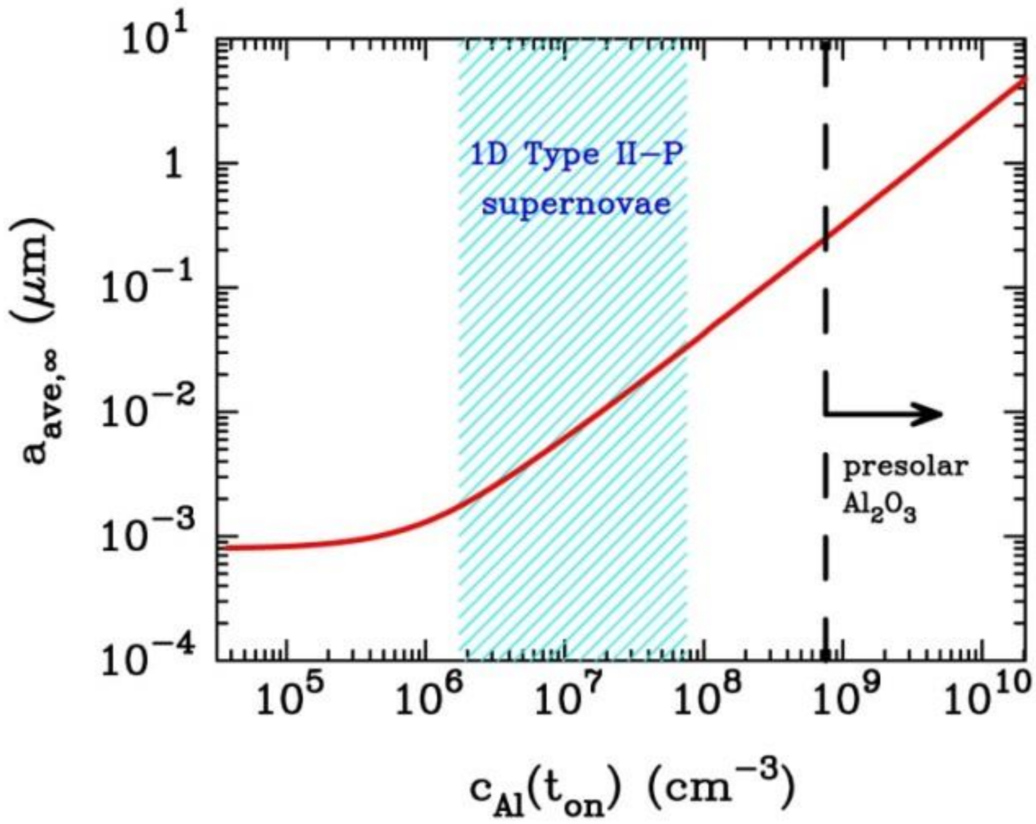

Nozawa+2015, ApJ, 811, L39

density of Al atoms at dust formation must be > ~10^9 cm^{-3}
➜ at least 10 times higher gas density than those predicted by 1-D SN models

Submicron-sized presolar Al_2O_3 grains identified as SN-origin were formed in dense clumps in the ejecta

4-5. Newly formed grains can survive in SNR?

Model of the calculation:

M_{SN}= (3 + 12) Msun, E_{exp}=1.8x10^{51} erg,

n_{ISM} = 1 cm^{-3}

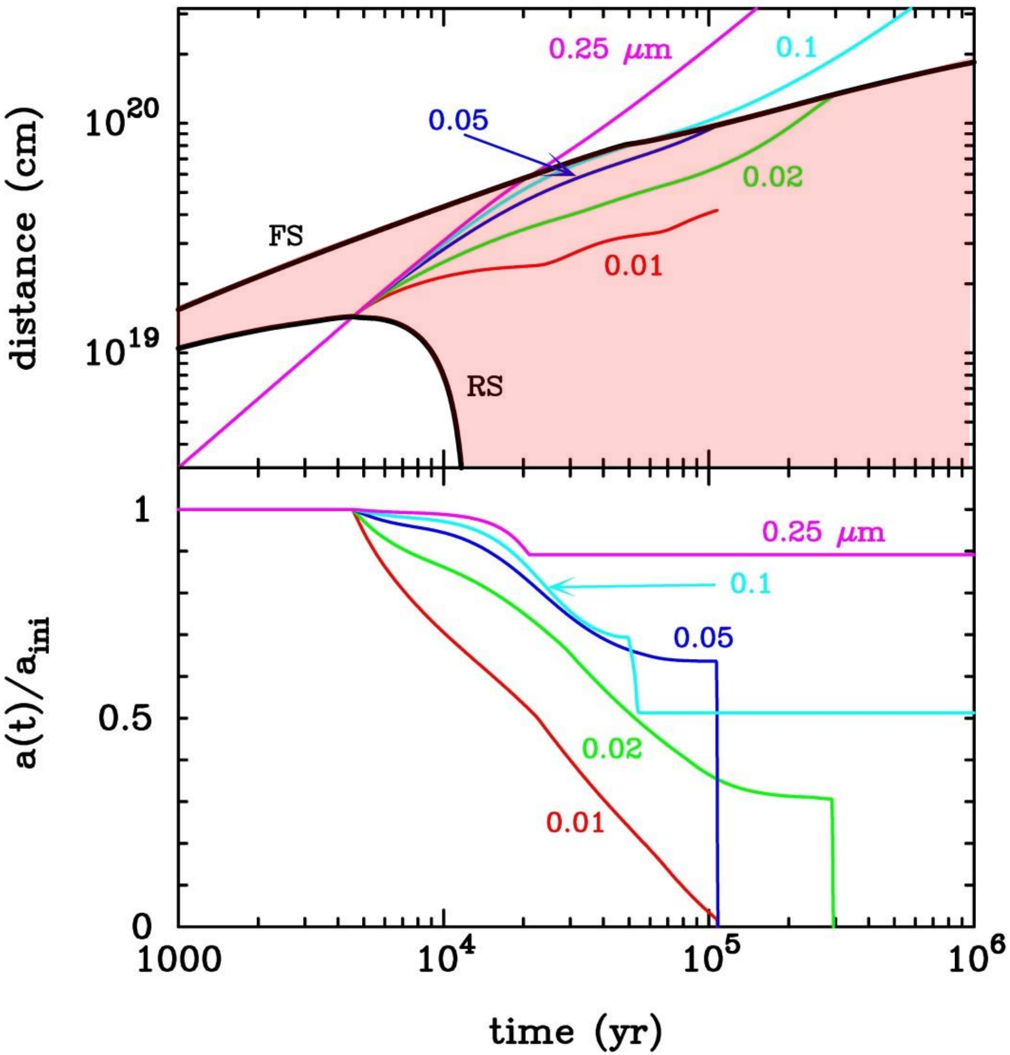

Nozawa+2015, ApJ, 811, L39

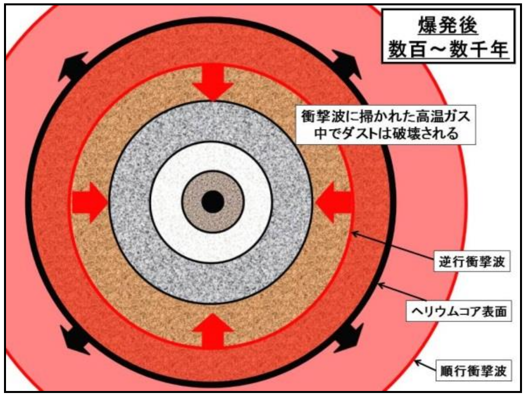

Evolution of dust in SNRs depends on the initial radii

- **a_{ini} < 0.01 μm**
  ➔ **completely destroyed**

- **0.02 μm < a_{ini} < 0.1 μm**
  ➔ **eroded in dense shell**

- **a_{ini} > 0.1 μm**
  ➔ **injected into the ISM**

4-6. Lifetimes of presolar grains in the ISM

○ Lifetimes of large grains against shattering in the ISM

$$\tau_{\rm VLG} = 1 \Big/ \frac{d\Phi}{dt}.$$

$$\frac{d\Phi}{dt} = \int_{a_{\rm min}}^{a_{\rm max}} F_{\rm sh} \frac{df_{\rm coll}}{da}\, da$$
$$= \int_{a_{\rm min}}^{a_{\rm max}} \pi(a_{\rm VLG} + a)^2 v_{\rm VLG} n(a) \frac{\phi}{1+\phi}\, da.$$

$$\phi = \frac{v_{\rm VLG}^2}{2Q_{\rm D}^{\star}} \frac{y}{1+y},$$

Hirashita, TN+2016, accepted, arXiv:1602.07094

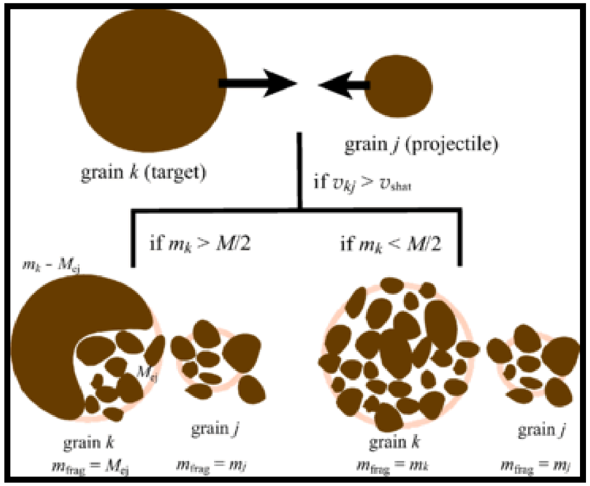

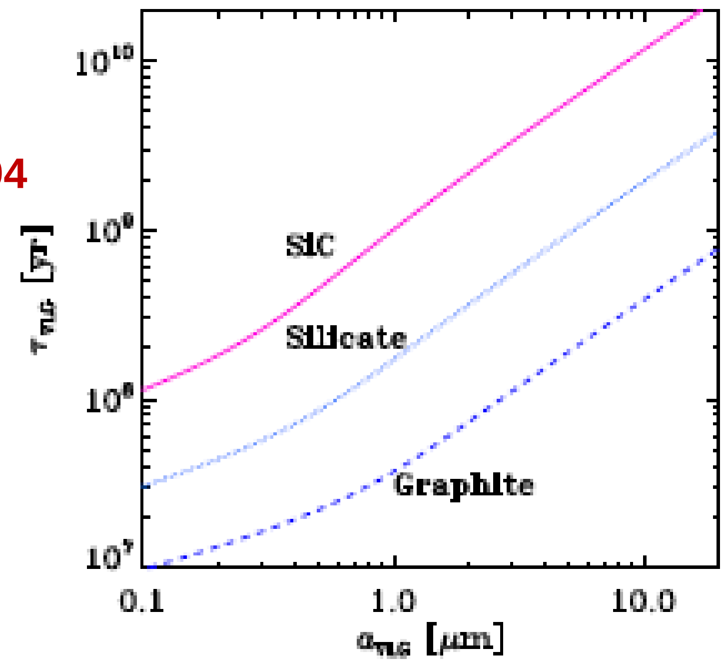

- Lifetimes of large grains increase with their initial radii

- SiC has a much longer timescale of destruction than silicate and graphite

4-7. Summary

1) SiC grains cannot form in the calculations because earlier formation of C grains consumes up the carbon atoms available for the formation of SiC.

2) Presolar Al_2O_3 grains with radii above 0.25 μm can be formed only in the gas with more than 10 times higher density than those estimated by 1-D SN models.
   ➜ indicating the presence of dense clumps in the SN ejecta

3) Lifetimes (shatterring timescale) of SiC grains above 0.1 μm in the ISM are longer than 10^8 year.

The measured sizes of presolar grains are powerful probes for constraining the physical conditions and processes in which they experienced.